The Evaluation of Fatigue Crack Propagation by Acoustic Emission

Jung-seob Hyun, Gee-wook Song, Bum-shin Kim, Soo-man Park
Korea Electric Power Research Institute, 103-16Munji-dong, Yusung-ku, Daejon, Korea

Abstract

Acoustic emission (AE) technique was used to investigate fatigue crack on compact tension specimens of aging materials at room temperature. Test materials have been used steam pipe under the actual operation conditions for a long time in fossil power plant.

The compact tension test specimens were subjected to load stress ratios of 0.33, 0.5, and 0.66. All the fatigue tests were performed at a frequency of 1Hz.

The test results indicate that acoustic emission count rates show reasonable correlation with crack propagation rates for applied stress ratios. When The crack growth rates increase, AE's counts and energies show increment. Also, the higher stress ratios, the faster crack propagation rates. Based on these relationships it may be possible to predict the remaining service life of fatigue-damaged steam pipes.

1. Introduction.

High-temperature pipes for power equipments include many welded parts. In particular, Reheat steam pipe has a large diameter and is produced by seam welding. Thus, damage on the welded parts is frequently reported and most of the cases resulted from cracks. If there is a crack in welded parts of a pipe, the crack grows further by fatigue. Then, it can lead to failure. In some cases, a crack can generate enormous economic loss and human injuries.

Non-destruction tests with UT, X-ray, and MT were the main conventional methods to detect a crack on high- temperature pipe. However, the existing method simply checks and assesses the status of equipments only when they are stopped for a long period. It can neither continuously check the equipments in operation nor reliably assess the status of a large pipe in a short time. Moreover, it takes much time and resources to inspect the pipe since the lagging materials around the pipe must be removed and reinstalled.

Acoustic Emission is a non-destructive evaluation technology that can tackle these problems. If a crack occurs or propagates further, Acoustic Emission technology evaluates the possibility of cracks and further developments by detecting elastic waves that are generated inside the material. Unlike conventional non-destructive tests, Acoustic Emission technology can inspect equipments in operation, detect a flaw from far distance, recognize locations, and monitor at any time given. Thus, it is an effective technology in inspecting and monitoring large equipments such as high- temperature pipes in fossil power plants. Moreover, it can minimize the negative impact from removal of lagging materials around the pipe so that it performs an effective inspection with economically low costs.

Therefore, to evaluate the initiation of fatigue crack and its growth by using Acoustic Emission technology, fatigue crack growth test was conducted according to stress ratios. This paper interpreted Acoustic Emission characteristics that are generated in crack growth and evaluated frequency of acoustic emission according to the growth rate of cracks and stress ratios.

2. Methods of the Test

We performed a crack growth test on DIN 13CrMo44, one of piping materials. Then characteristics of acoustic emission were examined and interpreted to figure out features of acoustic emission of the piping materials. Given the fact that actual piping materials have been exposed to high pressure and temperature for a long period, this study used materials that have been long operated in the power plant.

2.1. Test Materials

DIN 13CrMo44, which has been used as the main steam pipe for a long period of time, were designated as test materials. It's chemical composition and mechanical characteristics are showed in Table 1 and 2. Table 3 demonstrates operation conditions on piping, indicating that the material was used in high pressure and temperature for a long time.

Table 1 Chemical composition of test material.

	Comp.	C	S	Si	P	Mn	Cr	Mo
TestMaterial	wt(%)	0.178	0.017	0.334	-	0.586	0.735	0.699

Table 2 Mechanical characteristics of test material.

	Temp. (℃)	Young's Modulus (GPA)	Tensile Strength (MPa)	0.2% Yield Strength (MPa)	Elongation (%)
Test Material	24	205.1	484.1	280.7	33.8

Table 3 Operation condition of material.

Operation Temperature (℃)	Operation Pressure (kg/cm²)	Cycle	Operation Hours
515	92	487	185,000

The test specimen was extracted in a way that the notch tip was laid along the direction of length of the pipe so that the direction of the crack was vertical to circumference stress of the pipe. The specimen was produced as a compact tension based on the standard ASTM E647-99. Fig.1 shows the configuration of specimen.

2.2. Methods of the Test

The crack growth test was conducted by using oil-pressure fatigue tester (Instron Model 8521). Before the crack growth test, a crack was initiated on the specimen with a frequency of 5 Hz by using Sine waves with amplitude of 7KN. Then, pre-crack grew by 3mm after a gradual reduction of amplitude and frequency to 5KN and 1Hz, which were under the same condition of the test. The crack growth test was performed under the condition of amplitude of 5KN and frequency of 1 Hz. The load was applied to the stress ratio R of 0.33 for 5KN to 15KN, 0.5 for 10KN to 20 KN, and 0.66 for 20KN to 30KN.

To measure the length of the crack, compliance method was taken with a use of clip gauge. The measured length of the crack was precisely examined through comparison

with results measured by digital CCD microscope during the test. Then, the crack length was slightly revised after curve degree of the crack tip, shown in the specimen, was measured.

This test used Disp-24 of PAC for AE System, resonance sensor of 150khz, and wide range sensor ranging from 100khz to 1Mhz. Preamplifier was set to 40 dB, and threshold was 50 dB, at which noise got minimum, after measuring background noise of fatigue test machine before the test.[1][2]

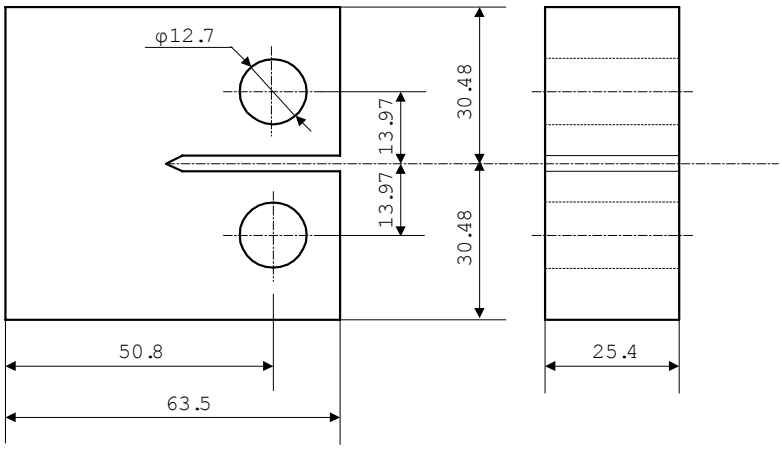

Fig. 1 Configuration of Specimen

3. Test Results and Conclusion

3.1. Results of Fatigue Crack Growth Test

Fig. 2 shows the growth of fatigue crack at R of 0.33, 0.5, and 0.66. The stress ratio can be demonstrated as R=P min/P max. This is the ratio of minimum load, in the lowest level of cyclic load, to maximum, in the highest level. Generally, the larger stress ratio is, the shorter the fatigue life lasts. In the Fig. 2, the fatigue life was 150,000 cycles at the stress ratio R of 0.33. However, the fatigue life was 130,000 cycles when R was 0.5, indicating the life was shorter in the case of the latter one. When stress ratio R was 0.66, initial crack growth rate was slower compared to the case of R of 0.33. However, the crack growth rate increased after the mid phase and the fatigue life was almost similar to the one with the R of 0.5. This seems to have resulted from inconsistency in material characteristics that the material was damaged from a long time of use in the power plant.

Fig. 3 shows the relations between crack growth rate, da/dN, and stress intensity factor range. Under the cyclic load, crack growth rate da/dN increases with the increase of stress intensity factor range, Δk. Δk = K max – K min (Kmin>0). In compact tension specimen, Δk can be calculated as following.[3]

$$\Delta K = \frac{\Delta P}{B\sqrt{W}} \int \frac{(2+\alpha)}{(1-\alpha)^{3/2}} (0.886 + 4.64\alpha - 13.32\alpha^2 + 14.72\alpha^3 - 5.6^4) \qquad (1)$$

where, $\alpha = a/W$, a is crack length, W is width of specimen

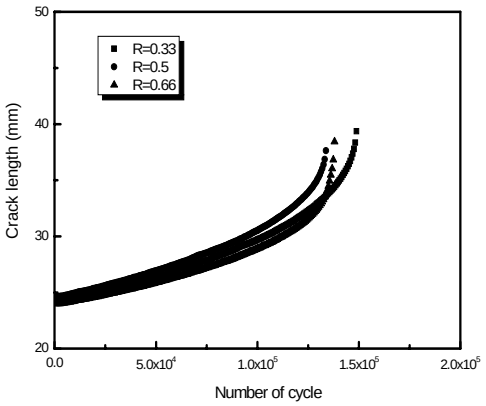

Fig. 2 Crack length versus number of cycle

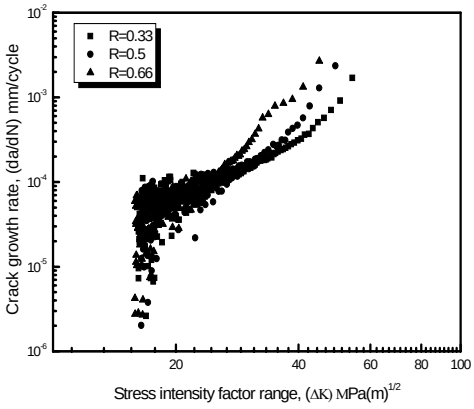

Fig. 3 Relation of crack growth rate and stress intensity factor range

Fig. 3 indicates that the crack growth was the fastest when stress ratio R was 0.66. Moreover, as the stress intensity is smaller, the crack growth rate slows down. Thus, stress ratio has a great influence on the crack growth ratio. However, the rate did not make much difference when stress intensity factor range Δk was small.

In general, in the range where stress intensity factor range is close to the minimum level, fracture surface ratio – a ratio that inter-granular fracture takes up on the surface of fracture - reaches to the maximum level. It is reported that this maximum point is equivalent to the transition point, where K and its around area are transferred to an area where da/dN and Δk have linear relations. In this case, Δk does not change even if stress ratio is different. Cyclic stress rather than mean stress plays a greater role in the crack growth.[4]

For these reasons, Fig. 3 explains that differences in crack growth speed according to different stress ratios are minor in the range where Δk was small, i.e., when stress intensity factor range was below 20Mpa-m1/2. Δk_{th} of the material is 18.5 Mpa-m1/2.

3.2. Characteristics of Acoustic Emission in the case of crack growth

When crack further propagated, acoustic emission signal was recorded. An acoustic emission sensor was installed on the specimen when fatigue test, which generates acoustic emission signals, was conducted. Fig. 4 shows the relations between fatigue cycle and AE cumulative counts. When the fatigue cycle increased, AE cumulative counts also increased. In specific, speed of increase in cumulative accounts was relatively slow in the initial period, very high in the middle, and moderate later on. Cumulative counts differ with the change of stress ratio. When stress ratio becomes greater, cumulative counts increase as well.

In Fig. 4, sharply increased cumulative counts are shown in the moderately increasing range in the latter part. It is likely that the material was internally ruptured at this point. This point is in between number of cycles 110,000 with stress ratio R of 5 and 80,000 cycles with R of 0.66. This can be interpreted as a big difference from Fig 2. in which rupture repetition number measured by clip gauge was 130,000 cycles with R of 0.5.

Clip gauge is installed in the front part of the test specimen to measure the crack opening displacement. Therefore, size of the crack can be measured only when the crack opening displacement increases with crack growth. In addition, time lag is

expected to occur until crack growth is to appear the crack opening displacement. Consequently, rupture number of cycles is belatedly calculated compared to acoustic emission signals that are generated with further crack growth in real time. It can be said that rupture number of cycles measured by acoustic emission signals more precisely reflects changes inside the material than the one by clip gauge.

Fig. 5 shows the relationship between cumulative energy of acoustic emission signals and number of cycles. The relations between the two are very similar to the one in Fig. 4 which cumulative counts and number of cycles is described. Also in Fig. 5, the range can be divided into three parts; slowly increasing part in the initial test, rapidly increasing one in the middle, and moderately increasing one afterwards. Cumulative energy differs according to stress ratios. The greater stress ratio is, the larger cumulative energy becomes. It is said that energy of acoustic emission signals have close relations with crack growth.

Therefore, it is likely that much of energy was emitted at R of 0.66 when crack growth ratio was high. In Fig. 5 as well as Fig. 4, a rapid increase of cumulative counts is demonstrated in the middle part. The rapidly increasing point is the rupture point of the test specimen. Ruptured number of cycles is identical to the one derived from Fig. 4. Thus, rupture of the material results in a surge of acoustic emission signal number and emission of much energy.

Fig. 6 and 7 show the relations between counts and number of cycles at stress ratio R of 0.5 and 0.66 respectively. The acoustic emission signals were more generated at high stress ratio. In Fig. 6, acoustic emission signals were the greatest when counts gradually increased and were ruptured as number of cycles increased. On the other hand, in Fig. 7, much of the acoustic emission signals were generated in a smaller number of cycle compared to rupture number of cycle. Fig. 7 can be compared to Fig. 3 that represents relations between crack growth ratio da/dN and stress intensity factor range. In the case of stress ratio R of 0.66, crack growth ratio rapidly increased at the stress intensity factor range of 30 to 36 Mpa-m1/2. Furthermore, many acoustic emission signals must have been generated in the range where crack growth ratio rapidly increased.

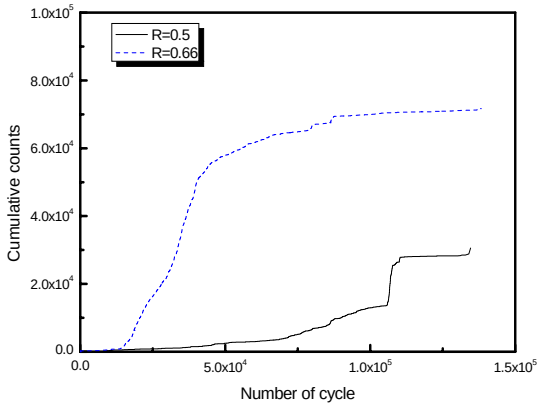

Fig. 4 Cumulative counts versus number of cycles

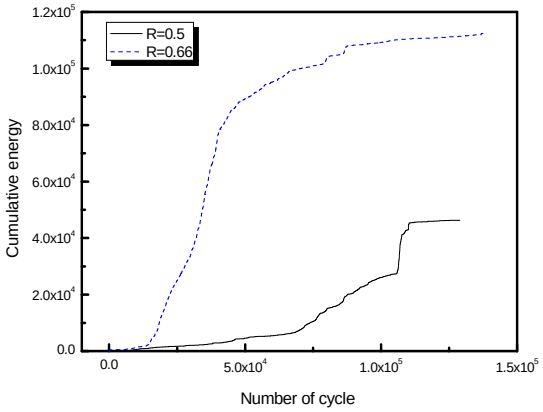

Fig. 5 Cumulative energy versus number of cycles

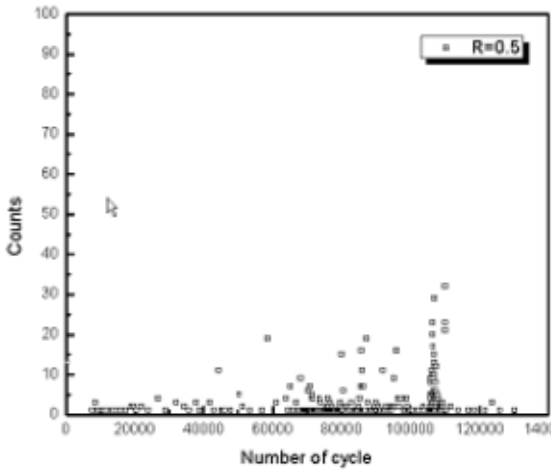

Fig. 6 Relation of counts and number of cycles for R=0.5

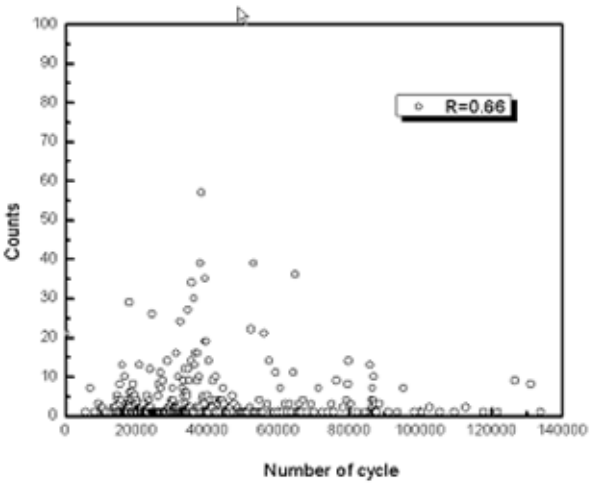

Fig.7 Relation of counts and number of cycles for R=0.66

Fig. 8 and 9 shows the relations between energy and number of cycles at stress ratio R of 0.5 and 0.66 respectively. More energy, which changed with numbers of acoustic emission signal, was generated as stress ratio increased. In addition, Fig. 9 explains that much of the acoustic emission energy was generated in the range where crack growth ratio enormously increased.

Fig. 10 and 11 shows the relations between amplitude and number of cycles at stress ratio R of 05 and 0.66 respectively. They demonstrate a similar pattern to Fig. 6 and 7. In Fig. 10 and 11, too, signals with larger amplitude were generated as stress ratio rose. As in Fig. 9, large amplitude was generated in the area where crack growth rate largely increased.

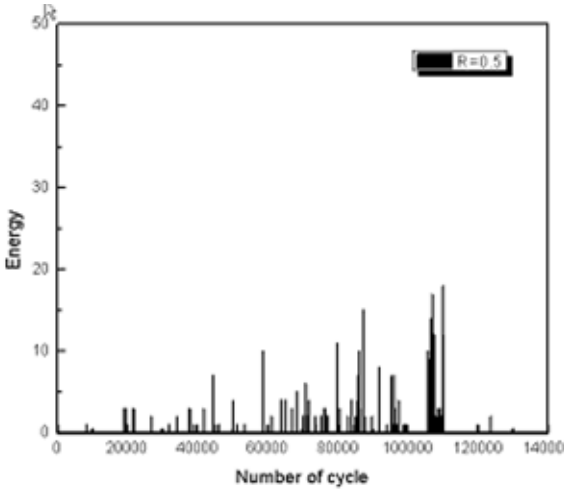

Fig. 8 Relation of energy and number of cycles for R=0.5

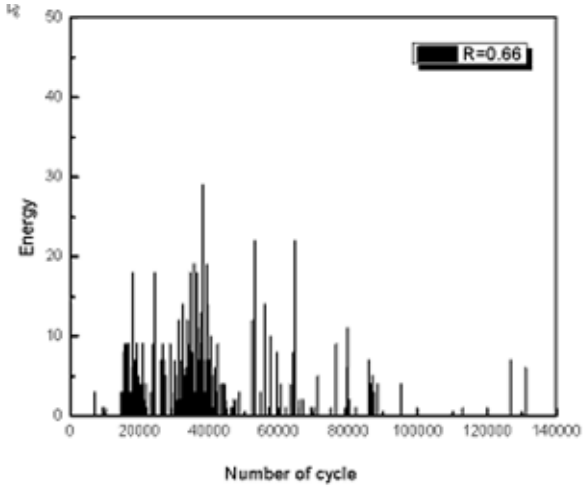

Fig. 9 Relation of energy and number of cycles for R=0.66

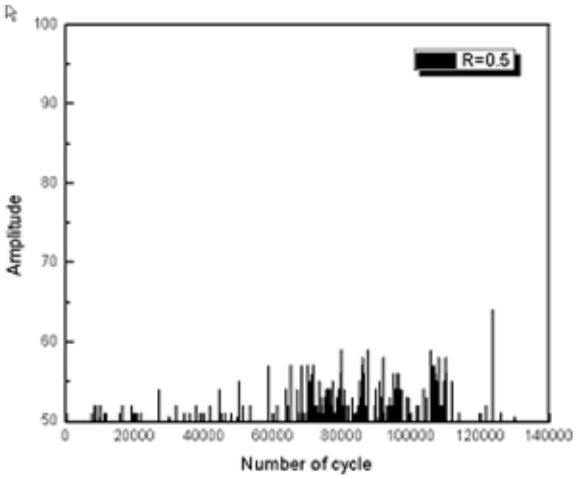

Fig. 10 Relation of amplitude and number of cycles for R=0.5

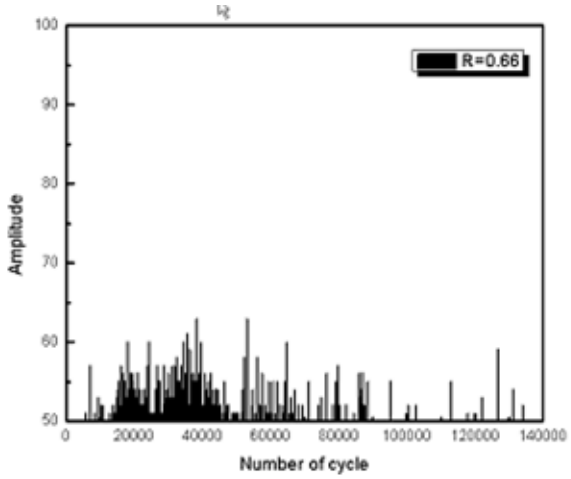

Fig. 11 Relation of amplitude and number of cycles for R=0.66

Fig. 12 and 13 represent the relations between amplitude of the signal and duration, when each stress ratio R is 0.5 and 0.66. When stress ratio becomes greater, amplitude of signal and duration increase.

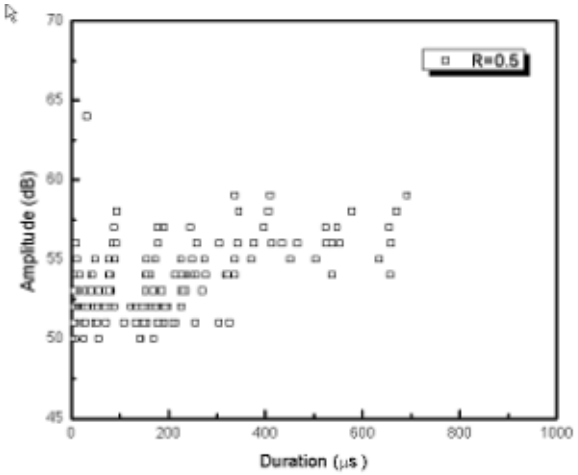

Fig.12 Relation of amplitude and duration for R=0.5

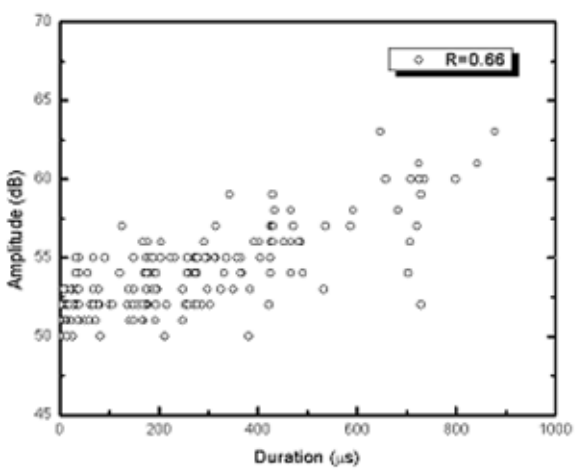

Fig. 13 Relation of amplitude and duration for R=0.66

4. Conclusions

This study conducted a fatigue crack growth test with changes of stress ratios, using a piping material that was used for a long period of time. Acoustic emission signals, generated in the case of crack growth, were obtained to interpret characteristics of acoustic emission in the case of crack growth and changes in the characteristics of acoustic emission with changes of stress ratios. The results of interpretation of the test can be concluded as following.

ⅰ) It was confirmed that crack growth ratio changed with changes of stress ratios. The difference of the ratio according to the changes of stress ratios did not appear in

Δk_{th} and its around area. However, the difference is apparently obvious in the area where da/dN and Δk have linear relations. Therefore, it is evaluated that stress ratio does not have much impact on the around area of Δk_{th}.

) The fatigue rupture point was precisely evaluated by acoustic emission method. The rupture on the test specimen was occurred in the area where acoustic emission signal number and energy rapidly increased. This indicates that acoustic emission signals clearly reflect changes inside the material.

) Acoustic emission signal number and energy increased when crack growth ratio rapidly increased. Therefore, it was confirmed that crack growth ratio can be evaluated by acoustic emission method.

References

1. T. M. Roberts, M. talebzzad, 2003, " Acoustic Emission Monitoring of Fatigue Crack Propagation," Journal of Constructional Steel Research, Vol 59, pp. 695-712.
2. John M. Rodgers, Bryan C. Morgan and Richard Tilly, 1996, "Acoustic Emission Monitoring for Inspection of Seam Welded Hot Reheat Piping in Fossil Power Plants," SPIE Conference on Nondestructive Evaluation Techniques for Aging Infrastructure & Manufacturing," Vol 2947.
3. ASTM E647-99, "Standard Test Method for Measurement of Fatigue Crack Growth Rates"
4. B. Tomkins, 1981, Fatigue; Introduction and Phenomenology, in Creep and Fatigue in High Temperature Alloys, Applied Science Publishers, pp. 73-113
5. Liptai, R. G., Ed., 1972, Acoustic Emission, ASTM STP 505, American Society for Testing and Materials
6. Spanner, J. C., Ed., 1975, Monitoring Structure Integrity by Acoustic Emission, ASTM STP 571, American Society for Testing and Materials
7. Cross, N. O., Loushin, L. L., and Thomson, J. L., 1972, Acoustic Emission, ASTM STP 505, American Society for Testing and Materials, pp. 270-296
8. Bryan C. Morgan and Richard Tilly, 1999, "Acoustic Emission Monitoring for Inspection of Power Plant Headers Utilizing Acoustic Emission Monitoring," NDT&E International, Vol 32, pp. 167-175.